NJC

FOCUS

View Article Online
View Journal | View Issue

Cite this: *New J. Chem.*, 2014, **38**, 1827

Shape-controlled synthesis of ruthenium nanocrystals and their catalytic applications

Guozhu Chen,† Jianming Zhang,* Akanksha Gupta, Federico Rosei and Dongling Ma*

Received (in Victoria, Australia) 24th September 2013,
Accepted 30th October 2013

DOI: 10.1039/c3nj01155k

www.rsc.org/njc

The catalytic properties of ruthenium (Ru) are fairly well known. Nevertheless its shape-controlled synthesis (especially as compared to other noble metals) is still elusive. In this review, we present recent advances in the synthesis of Ru nanomaterials, in particular, spherical nanoparticles, one dimensional nanostructures, nanoplates and hollow structures, as well as other examples. In addition, the catalytic applications of Ru materials are selectively surveyed. Finally, the challenges and perspectives on the controlled synthesis of Ru-based nanomaterials and their catalytic applications are described.

1. Introduction

The synthesis of noble metal nanostructures has been a hot topic for decades because of their various important applications, such as catalysis, bioanalysis and optics.[1–4] It is well-known that the properties of a noble metal are determined by a set of physical parameters including size, shape, and composition.[1–3] Considerable research efforts have been devoted to the control of shape, because it allows one to fine tune the properties with greater versatility than what can be achieved otherwise. For example, triangular Ag nanocrystals have been used as effective substrates for surface enhanced Raman scattering (SERS) in the spectral range of 700–800 nm, while spherical Ag nanoparticles (NPs) are most suitable for SERS in the range of 530–570 nm.[4] Another quintessential example is given by Pt-catalyzed hydrogenation of benzene: Pt with surfaces enclosed by {100} facets yields only cyclohexane while Pt enclosed by {111} facets leads to both cyclohexene and cyclohexane.[5] Although the shape-controlled synthesis of noble metals has been well documented, it has mainly been focused on Ag, Pt, Pd, Au with the face centered cubic (fcc) crystal structure.[1–3] For those with the hexagonal closed packed (hcp) structure, *e.g.* ruthenium (Ru), their shape-controlled synthesis is still in its infancy.

Ru, as a well-known catalyst, has been the focus of considerable attention in catalytic reactions, such as selective hydrogenation, dehydrogenation of ammonia borane (AB), CO oxidation, and many more.[6–12] In addition to showing excellent catalytic activity, as compared to other noble metals, such as Pt and Au (~$1300–1500/oz), Ru (<$100 USD/oz) is much less expensive. So far, various methods have been successfully employed in shape-controlling of fcc structured noble metals, however, those methods cannot be readily extended to synthesize hcp structured Ru nanomaterials, although fcc structured Ru has been reported recently.[13] Therefore, both shape-controlled synthesis of Ru nanomaterials and the understanding of their corresponding growth mechanisms remain important challenges.

Ru nanocrystals can be synthesized by either solution-phase or gas-phase methods. This review will focus on solution-phase methods, due to space limitations. Attributed to the high standard redox potential of Ru, Ru nanostructures can be easily obtained by the reduction of Ru precursors with various reductants, like $NaBH_4$,[14] polyols,[10,13,15] and even AB[21] with weak reducing ability. To effectively control the size and shape, capping agents are normally employed. Alternatively, Ru nanocrystals can also be synthesized by the decomposition of an organometallic complex, such as $Ru_3(CO)_{12}$.[9,22,23] Under these synthetic methods, size-controlled and/or shape-controlled synthesis of Ru nanocrystals has been acquired by tuning different reaction variables including the type of metal precursors, solvents, temperature, and capping agents.

2. Shape controlled synthesis of Ru nanostructures

2.1 Synthesis of spherical Ru NPs

Since catalytic properties are strongly dependent on the size and shape of solid particles, their use as advanced materials in high technology or as model materials in fundamental studies requires non-agglomerated and mono-dispersed particles with uniform size and shape distribution. For this purpose, NPs are

Institut National de la Recherche Scientifique (INRS), 1650 Boulevard Lionel-Boulet, Varennes, Québec J3X 1S2, Canada. E-mail: ma@emt.inrs.ca, zhangjm@emt.inrs.ca; Fax: +1-450-929-8102; Tel: +1-514-228-6920

† Currently, Key Laboratory of Fluorine Chemistry and Chemical Materials of Shandong Province, School of Chemistry and Chemical Engineering, University of Jinan, 336 Nanxinzhuang West Road, Jinan, Shandong, 250022, China. E-mail: chm_chengz@ujn.edu.cn.

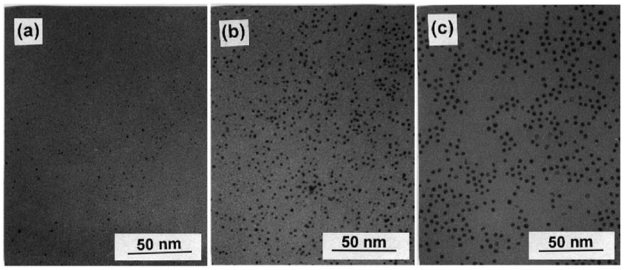

Fig. 1 Transmission electron microscopy (TEM) images of Ru NPs prepared in sodium acetate solution. (a) d_m = 1.4 nm; (b) d_m = 2.5 nm; and (c) d_m = 3.5 nm. Adapted from ref. 15. Copyright 2003 American Chemical Society.

usually stabilized *via* the addition of surfactants, polymers, or ligands to avoid NP agglomeration and to control NP morphology. For example, uniform Ru NPs with a tunable particle size (d_m) from 2 to 6 nm (Fig. 1) were synthesized by the polyol reduction of $RuCl_3$ in the presence of poly(vinylpyrrolidone), and the particle size could be tuned by varying the reaction temperature and the acetate ion concentration.[15] Highly stable water-soluble Ru NPs (d_m: ~1.6 nm) were synthesized using a sulfonated diphosphine-cyclodextrin supramolecule as a stabilizer.[16] With nitrocellulose or cellulose acetate polymers as stabilizers, Ru NPs (d_m: 1–2 nm) could also be synthesized by reducing Ru(1,5-cyclooctadiene)(1,3,5-cyclooctatriene) (Ru(COD)(COT)) under H_2 at room temperature.[17] Ionic-liquids (ILs), as a replacement of usual solvents, have also been used to prepare Ru NPs. The ILs demonstrate dual functions in the synthesis, acting both as dispersion media and stabilizer.[18] For example, small Ru NPs (~2 nm) were synthesized in nitrile-functionalized ILs using a Ru complex, and were stabilized by ILs *via* nitrile bonding.[19] Their unique tri-dimensional network structure exerts important confinement effect on NP growth and stabilization.[18] Nevertheless, the presence of these stabilizers on the NP surface can strongly influence the physical and chemical properties of NPs, *e.g.* obstructing the access of reactants to the active sites of NPs and thus decreasing their catalytic activity. Support materials are also widely used as another effective strategy to stabilize NPs. Recently, our group reported Ru nanoclusters (~1.7 nm) supported on carbon black from the reduction of $RuCl_3$ by AB. The carbon black is responsible for the stabilization and immobilization of well dispersed Ru clusters.[21] In addition, a thermal reduction method for preparing Ru catalysts supported on various carbon-based substrates was also demonstrated, where the carbon species in substrates could thermally reduce Ru precursors at high temperature, resulting in Ru NPs with good dispersion, high crystallinity, and strong resistance against an oxidative atmosphere, yet without causing any pore blocking problems.[8] Oxides have also been used as supports for Ru NP synthesis. For instance, using an impregnation-dry reduction method, [Ru(COD)(COT)] precursors loaded on mesoporous silica were decomposed at room temperature to form well dispersed Ru NPs.[20] The significant convenience of this approach lies in the omission of thermal treatment due to the mild reduction conditions and the stabilization of the NPs by suitable pores of oxides.

Apart from the conventional synthesis methods discussed above, there have been certain reports on the synthesis of Ru NPs supported on different materials by a microwave irradiation route.[24–27] The microwave irradiation method is emerging as a promising approach for rapid and large-scale synthesis of high-quality nanocrystals. For example, uniform Ru NPs (2.2 ± 0.4 nm) were successfully synthesized and well dispersed on chemically derived graphene (CDG) by microwave irradiation of $Ru_3(CO)_{12}$ in a suspension of CDG in 1-butyl-3-methyl-imidazolium tetrafluoroborate for 6 min.[24] In another study, facetted Ru NPs were synthesized and deposited onto carbon nanotubes (CNTs) by irradiating $Ru_3(CO)_{12}$ in the presence of CNTs. With the irradiation time increasing from 1 to 5 min, both NP size and crystallinity clearly increased.[27]

2.2 Synthesis of one-dimensional (1D) Ru nanostructures

1D structures have been promoted as an exciting new structural paradigm for catalysis because 1D architectures possess several unique inherent advantages. For the metals with the hcp crystal structure, growth is generally favoured in the direction of the *c*-axis due to intrinsic anisotropy, eventually leading to 1D nanostructures.[28] In the case of 1D Ru nanomaterials, however, more investigations are required. In fact, only a few reports, to the best of our knowledge, have so far demonstrated the synthesis of 1D Ru nanomaterials. For example, Rao *et al.* synthesized Ru nanorods with a length of 50 nm and an average diameter of 15 nm by carrying out the decomposition of $Ru(acac)_3$ in *n*-octylamine at 320 °C. They proposed that the alkylamine medium dictated the shape of the nanostructure and favoured the rod shape.[29] Besides that the uniformity of the shape of the Ru nanorods needs to be further improved, the high reaction temperature (>300 °C) may be another challenge in terms of their practical applications. With the assistance of the hard template of a porous aluminum oxide (AAO) membrane, Guay *et al.* prepared Ru 1D nanowires and nanotubes *via* electrodeposition. Micrometer-long nanowires and nanotubes showed an outer diameter of *ca.* 200 nm, close to the inner diameter of the porous AAO membrane.[30] More recently, high-quality, crystalline Ru nanowires were achieved using a simple, ambient, template-based method (Fig. 2).[14] They were synthesized by the reduction of K_2RuCl_6 with $NaBH_4$ within the pores of a commercially available polycarbonate (PC) membrane. The nucleation and growth of metallic Ru occurred within the spatially confined regions of the anisotropic 1D pores of the PC membrane, thereby leading to the generation of highly anisotropic nanostructures.

2.3 Synthesis of Ru nanoplates

Noble metal nanoplates, as a new class of two-dimensional nanostructures, exhibit fascinating properties such as intense quadrupole plasmonic resonance, and have been used for both chemical and biological sensing and catalytic applications.[31] Generally, slow formation of zero-valence metal atoms and preferred growth in certain crystallographic directions by altering kinetic parameters, *e.g.* by choosing appropriate facet-selective-adsorbing agents, are essential to obtain noble metal nanoplates. For example, through the reduction of $RuCl_3 \cdot xH_2O$ by formaldehyde (HCHO)

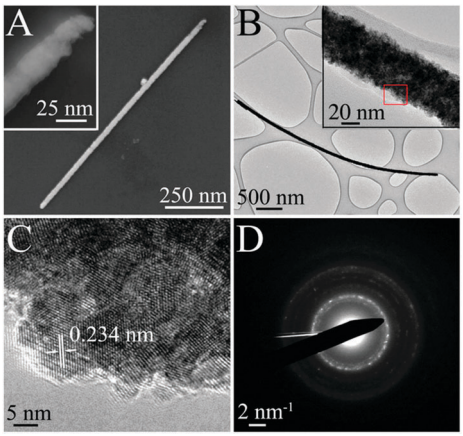

Fig. 2 Scanning Electron Microscopy (SEM) (A) and TEM (B) images of individual, isolated Ru nanowires. Higher-magnification SEM and TEM images are shown as insets. High resolution TEM (HRTEM) (C) and Selected-Area Electron Diffraction (SAED) (D) patterns were obtained from a representative area of the central region of a typical wire, as designated by the red box. Reprinted with permission from ref. 14. Copyright 2013 American Chemical Society.

in a hydrothermal process, Zhang and Yan successfully prepared triangular and irregular Ru nanoplates, and capped columns with high shape selectivity as demonstrated in Fig. 3.[32] On the basis of their experimental results and density functional theory (DFT) calculations, they found that both the intrinsic characteristics of Ru crystals and the adsorption of certain reagents are responsible for the final shape of Ru nanocrystals. Specifically, due to the selective adsorption of oxalate species on Ru $(10\bar{1}0)$ and the lower surface energy of Ru (0001), both triangular and irregular Ru nanoplates exposed a large portion of (0001) facets.

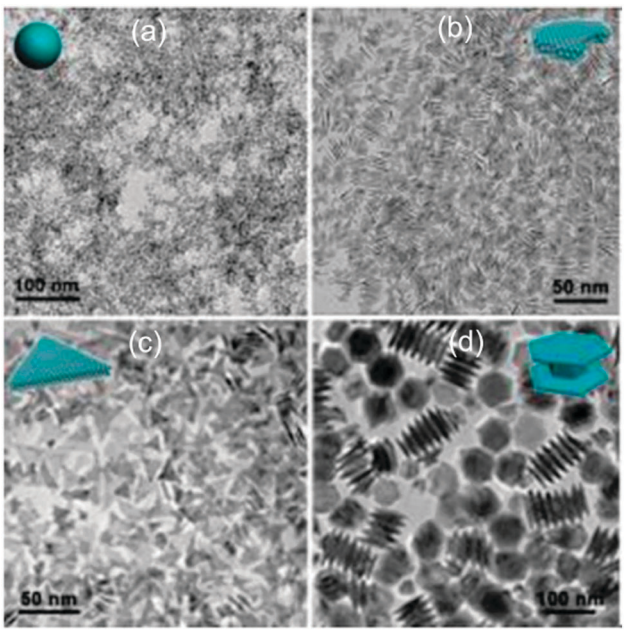

Fig. 3 Ru nanostructures of spheres (a), irregular plates (b), triangular plates (c), and capped columns (d). Reprinted with permission from ref. 32. Copyright 2012 American Chemical Society.

With the reaction proceeding, the effect of selective adsorption disappeared due to the gradual thermolysis of the oxalate species, leading to the shape evolution of Ru nanocrystals from prisms to capped columns. More interestingly, they found that the SERS signals of these Ru nanocrystals with 4-mercaptopyridine as molecular probes showed an enhancement sequence of capped columns > triangular nanoplates > nanospheres, and proposed that sharp corners and edges in the capped columns and nanoplates as well as the shrinking interparticle distance in their assemblies are responsible for observed differences in their properties.

2.4 Synthesis of hollow Ru NPs

Hollow structures made of noble metals are intriguing since this kind of structures has high surface area and maximizes the precious element's surface to volume ratio. Recently, our group synthesized hollow metallic Ru NPs (Fig. 4b) with small diameter (~14 nm) and thin wall (~2 nm) using Ni NPs as templates. The thin Ru shell was first deposited onto the surface of Ni NPs to form uniform Ni@Ru core@shell NPs (Fig. 4a) *via* the thermal decomposition of $Ru_3(CO)_{12}$, and then the Ni templates were removed by acid etching. We found that the presence of surface ligands and an inert atmosphere are responsible for effectively protecting the Ru NPs against oxidation.[9] Recently, a general strategy for the synthesis of noble metal NPs, including Ru, with

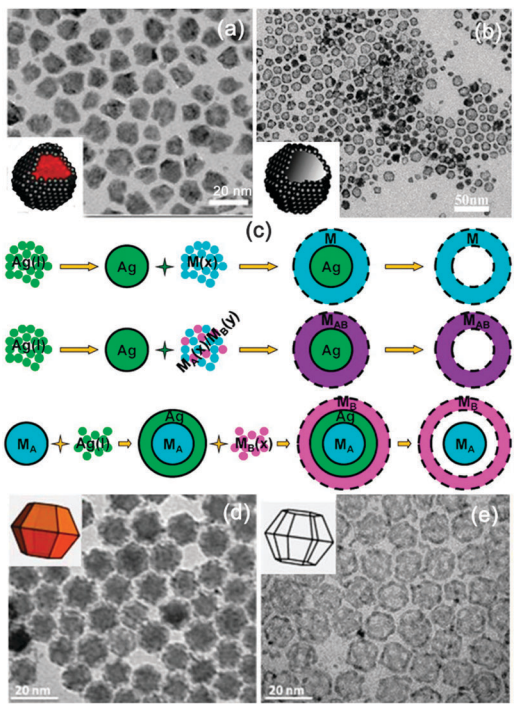

Fig. 4 TEM images of Ni@Ru core@shell (a) and hollow Ru NPs (b). Reproduced from ref. 9 with permission from the Centre National de la Recherche Scientifique (CNRS) and the Royal Society of Chemistry. (c) Scheme of the synthetic route of hollow or cage-bell metal structures using Ag NP template. Reprinted with permission from ref. 33. Copyright 2012 American Chemical Society. TEM images of Cu_2S@Ru core@shell structure (d) and Ru nanocages (e). Adapted from ref. 34 with permission from Macmillan Publishers Ltd: *Nature Mater.*: **9**, 810. Copyright 2010.

hollow or cage-bell structures was reported. It was based on the diffusion of Ag cores and their interaction with the bis(*p*-sulfonatophenyl)phenylphosphane dehydrate dipotassium salt, which binds strongly to Ag(I)/Ag(0) to promote the inside-out diffusion of Ag in the Ag@M core@shell structures (Fig. 4c).[33] The hollow structured Ru nanocages (Fig. 4e) were also realized by leaching copper sulphide with a solution of neocuproine in chloroform after selective growth of Ru on the crystal edges of the Cu_2S seeds into Cu_2S@Ru NPs (Fig. 4d). The formation of the unique cage structures differs from the most commonly observed island growth mode of hybrid NPs. The faceting of the Cu_2S seed particles that provide sharp edges for the reaction is responsible for the unique cage formation. In addition, passivating ligands of thiols on these well-defined facets strongly bonded to the surface of the Cu_2S particles, blocking the growth of the surface while only leaving the higher energy edges as the preferred reaction sites for the redox reduction of the metal. The role of the thiol ligands was thus also taken into consideration for discussing Ru cage formation.[34]

2.5 Synthesis of Ru nanomaterials with other morphologies

Apart from shapes mentioned above, Ru nanomaterials with star and branch structures were also synthesized through the decomposition of $Ru_3(CO)_{12}$ in the presence of different organic stabilizers.[22,23] For example, Ru NPs with a diameter of ~6 nm were synthesized in the presence of polyvinylpyrrolidone (PVP),[41] while faceting and branching Ru nanocrystals were prepared when tri(*n*-octyl)amine was used as a stabilizer;[22] Ru nanostars and nanourchins can also be achieved in toluene at 160 °C under hydrogen atmosphere in the presence of hexadecylamine.[23] The stabilizers play an important role during the Ru nanostructure growth process. The ability of the different stabilizing molecules to preferentially stabilize certain facets is believed to be responsible for controlling these kinds of shapes.[22] More recently, hourglass-shaped Ru nanocrystals were synthesized by reacting $Ru(acac)_3$ with 3 bar of hydrogen in a Fischer–Porter bottle.[35] Dodecylamine was employed as the organic stabilizer. The hourglass nanocrystal was bound by {001} and {101} facets at the ends and sides respectively, different from the Ru nanoplates introduced above, where selective adsorption of capping ligands on the (001) hcp facets occurred. Since (001) and (101) facets can accommodate a more dense coverage of dodecylamine, the favourable adsorption on these specific facets must be energy dictated as it can lead to larger reduction in the surface energy of the nanocrystals. However, when either oleyamine or hexadecylamine was applied, irregular shaped nanocrystals were achieved possibly due to their weaker ability for surface stabilization, which indeed requires more investigations. Once again, one thing is certain that ligands play an important and subtle role in shape controlled synthesis of Ru nanocrystals (Fig. 5).

In addition, Ru-based bimetallic nanomaterials are also of particular interest because they are expected to exhibit remarkable properties distinctly different from their monometallic counterparts. The well-known example is Ru–Pt bimetallic nanomaterials, which exhibit outstanding performance for the electrooxidation of both H_2 and methanol.[36] The 1D structured Ru–Pt nanomaterials have been prepared by template-assisted approaches.[37,38] Ru–Pt nanomaterials with hollow and mesoporous structures have also been reported.[39,40] Among Ru-based bimetallic structures, M@Ru core@shell structure is worthwhile to note because this configuration maximizes the precious element's surface to volume ratio with significant economic advantages. For example, Ni@Ru core@shell NPs were synthesized by means of a seeded growth method, where the Ni NPs were pre-synthesized, followed by the decomposition of $Ru_3(CO)_{12}$ in oleylamine.

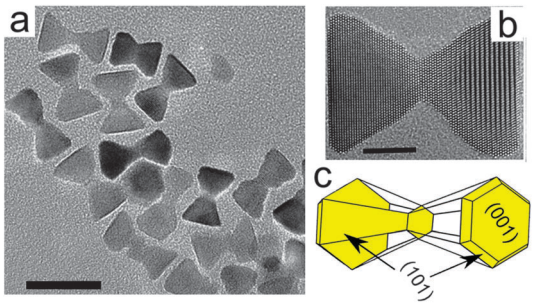

Fig. 5 (a) TEM image of Ru hourglass nanocrystals, scale bar = 20 nm. (b) HRTEM image of a single, highly crystalline Ru hourglass nanocrystal, scale bar = 5 nm. (c) Schematic of a single Ru hourglass nanocrystal showing structural termination by {001} and {101} facets. Adapted from ref. 35. Copyright 2013 American Chemical Society.

3. Catalytic applications

3.1 Hydrogenation

It is well known that Ru exhibits a unique, increased selectivity toward hydrogenation of a carbonyl group in the vicinity of a C=C double bond (either isolated or conjugated) or an aromatic ring.[16,19,20] The typical properties of the Ru catalysts in the hydrogenation reactions were reviewed by Libor Cerveny.[42] It is proposed that basically the reaction catalyzed by Ru NPs proceeds in four steps: (i) adsorption/dissociation of hydrogen on the catalytically active sites of the NPs; (ii) adsorption/dissociation of molecules with a C=C bond on the NP surface; (iii) hydrogenation reaction between adsorbed molecules and surface-hydrogen; (iv) desorption of products from the NP surface. Usually the adsorption or desorption rate determines the catalytic reaction efficiency.[42] It was found that supports, modifiers of catalysts, NP size and structure (monometallic or bimetallic) are all important factors governing the catalytic selectivity and activity of the catalysts. For example, Zhao *et al.* synthesized Ru NPs supported on various carbon-based substrates, which exhibited excellent catalytic performance attributed to the intimate interfacial contact between Ru NPs and the carbon support.[8]

3.2 Ammonia synthesis

The synthesis of NH_3 is probably the most studied reaction in heterogeneous catalysis, and Ru is known to exhibit one of the highest catalytic activities for ammonia synthesis. Again, in this

reaction, the catalytic activity of supported Ru is closely related to preparation methods, and the morphology (*i.e.*, size, shape, *etc.*) of such prepared particles. The support was also found to have a large effect. For example, active carbon materials are well known supports for Ru and carbon supported Ru catalysts have been commonly used in commercial ammonia plants.[43] Bao *et al.* recently employed CNTs as a new support and found that the catalyst with Ru NPs dispersed almost exclusively on the exterior CNT surface exhibited a higher activity than the CNT-confined Ru (*i.e.*, Ru NPs dispersed inside CNT channels) due to the higher electron density of outside Ru than that of inside Ru.[11]

3.3 Dehydrogenation of AB

AB (NH_3–BN_3) has been identified as one of the leading molecular candidates for hydrogen storage. Hydrogen can be achieved by the hydrolysis of AB in the presence of a catalyst. Among all catalysts reported, Ru NPs are most studied for AB dehydrogenation. The high price and limited abundance of Ru, however, hinder their practical applications. It is therefore desired to improve their activity and simultaneously minimize the use of Ru. Recently, our group successively prepared Ni@Ru core@shell NPs,[41] Ni–Ru alloyed NPs,[44] hollow Ru NPs,[9] and carbon black supported surfactant-free Ru nanoclusters,[21] and studied their catalytic performance during the hydrolysis of AB. As shown in Fig. 6, the Ni–Ru alloy NPs exhibited higher catalytic activity than the Ni@Ru core@shell NPs and both were more active than similar sized monometallic Ru NPs. In the Ni@Ru core@shell structure, significant enlargement of the surface area of Ru and synergistic Ru–Ni interactions are considered as reasons for their enhanced catalytic activity in dehydrogenation of AB and the existence of Ni cores endows the NPs with magnetic property as well.[41] In the case of Ni–Ru alloy NPs, it is proposed that the structure of Ru islands surrounded by Ni atoms on the NP surface was formed, and the strong synergistic effect between Ni and Ru in the alloy NPs is believed to account for their superior catalytic activity.[44]

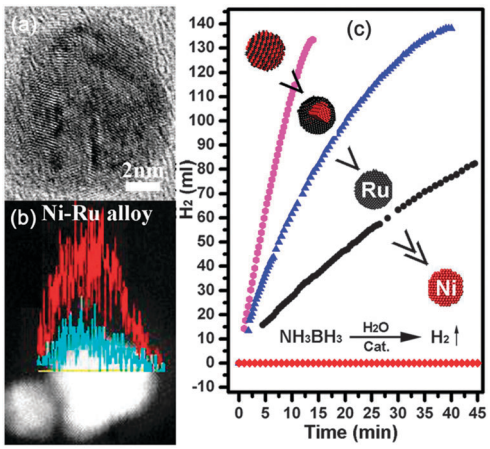

Fig. 6 (a) HRTEM image of a single $Ni_{0.74}Ru_{0.26}$ alloy NP; (b) Ni and Ru compositional-line profiles recorded along the median line of a single particle in the scanning transmission electron microscope image; (c) comparison of catalytic activities of monometallic Ni, monometallic Ru, Ni@Ru core@shell, and Ni–Ru alloy NPs for AB hydrolysis at 30 ± 1 °C. [Ru] = 0.25 mM in monometallic Ru, in Ni@Ru, and in Ni–Ru alloy NPs; for monometallic Ni, [Ni] = 1 mM; [AB]: 200 mM; volume of the dispersion = 10 mL. Adapted from ref. 44. Copyright 2013 Wiley-VCH Verlag.

3.4 CO oxidation

CO oxidation is of practical importance in many industrial processes, such as the removal of CO from automobile exhaust gases and preferential CO oxidation to purify hydrogen for its use as a clean and effective fuel in fuel cells. Of the noble metal catalysts, Ru has shown an unusual catalytic behaviour for CO oxidation. For example, the Ru single crystal surface is the least active among noble metals under ultrahigh vacuum conditions, while it turns out to be highly active under oxidizing and high pressure conditions. The influence of Ru particle size on CO oxidation was reported by Joo's group. They carried out CO oxidation on Ru NPs ranging in size from 2 to 7 nm, and found that the catalytic activity increased as the size of the Ru NPs increased. The formation of Ru oxide on the surface plays a great role during the CO oxidation: smaller Ru NPs would be subjected to a higher degree of oxidation than larger ones, thus exposing less catalytically active sites on their surfaces.[10,45] The crystalline structure of NPs also has important impact on catalysis. Very recently, Kitagawa *et al.* synthesized γ-Al_2O_3 supported fcc-Ru NPs, which yielded remarkably higher catalytic activity in CO oxidation than hcp-NPs.[13]

3.5 Other catalytic applications

Ru catalysts are also widely used in other catalytic reactions. For example, Ru NPs supported on CNTs display promising catalytic performance for selective conversion of syngas to diesel fuel.[46] Water-soluble Ru(0) nanoclusters have also been employed for aqueous-phase Fischer–Tropsch synthesis;[12] With regard to Ru–M, especially Ru–Pt bimetallic NPs, they have demonstrated excellent catalytic activity in the applications of fuel cells[43] and elimination of environmental pollutants.[47] In particular, the presence of Ru can alter the electronic properties of Pt, known as the ligand effect, thus causing CO to adsorb less strongly on the catalyst surface during CO-involved reactions. It can also provide oxygen-containing species at more negative potentials than Pt, which enables the CO oxidation on adjacent Pt sites following the so-called bifunctional mechanism.[40]

4. Conclusions and perspectives

This review highlights the recent progress in the shape controlled synthesis of mono-/bi-metallic Ru nanomaterials. Some typical catalytic applications regarding Ru have also been briefly introduced. Although considerable attention has been devoted to the synthesis of Ru nanomaterials in the past years, in comparison to other noble metals, there is still much more room to make progress in shape-controlled synthesis of Ru mono-/bi-metallic nanomaterials. From the synthesis viewpoint, exploring suitable kinds of reductants and/or facet-selective adsorption agents is still the first choice to realize the controlled synthesis of Ru nanocrystals with well-defined morphologies.

Different preparation approaches also provide the possibility to achieve various morphologies. In the case of Ru-based bimetallic nanomaterials, additional factors should be taken into consideration during their synthesis: cohesive energy, surface energy, atomic radii, electronegativity, standard redox potentials, and crystal structure difference between Ru and the second metal. These factors definitely raise the difficulty in the morphology-controlled preparation of Ru-based bimetallic nanomaterials. From the catalytic performance viewpoint, additional work is still required to thoroughly explore the correlation between morphology (in particular, certain crystal planes) and catalytic activities. Future studies should be focused on (1) shape-controlled synthesis of Ru mono-/bi-metallic nanomaterials with desired crystal facets and different dimensions; (2) studying the surface structure dependent catalytic activity, which would build a solid foundation for tuning and optimizing catalytic performance following the so called "function follows form" mantra; (3) using DFT calculations to provide insights into the rational design of Ru-based catalysts with high activity and understanding their surface reaction mechanisms and kinetics during catalytic reactions; and beyond that, (4) further studying the synergistic effect in the Ru-based bimetallic structure and the interactions between Ru-based NPs and the support. Since Ru is a precious metal, it is also important to bear in mind the overall economic cost during new catalyst development. Some encouraging results have been achieved in terms of decreasing Ru use by increasing the catalytic efficiency of Ru-based catalysts *via* forming Ru-based bimetallic structures. Nonetheless, (5) the realization of more economical Ru-based catalysts (*e.g.* a cheap-metal-core@monolayer-Ru-shell structure) by developing simple, cost-effective, large-scale synthesis and fabrication processes is still highly desired and essential for expanding their practical applications. In this regard, microwave-synthesis appears promising considering its unique features of uniform heating, high efficiency, environmental friendliness, *etc.* In short, Ru-based nanomaterials will play a more important role in catalysis upon gaining further insights into their synthesis and properties.

Acknowledgements

We acknowledge funding from NSERC through Discovery Grants to D.M. and F.R. and a Strategic Project Grant. D.M. thanks financial support from FQRNT. F.R. is grateful to the Canada Research Chairs program for partial salary support. We are grateful to the Agence de l'Efficacite Energetique for supporting part of this work. The authors would like to thank Prof. R. Rosei for helpful discussions on catalytic reactions and for several years of collaborative work on nanostructured catalysts.

Notes and references

1 Y. Xia, Y. Xiong, B. Lim and S. E. Skrabalak, *Angew. Chem., Int. Ed.*, 2009, **48**, 60–103.
2 A. R. Tao, S. Habas and P. Yang, *Small*, 2008, **4**, 310–325.
3 B. Wiley, Y. Sun, B. Mayers and Y. Xia, *Chem.–Eur. J.*, 2005, **11**, 454–463.
4 L. A. Dick, A. D. McFarland, C. L. Haynes and R. P. Van Duyne, *J. Phys. Chem. B*, 2002, **106**, 853–860.
5 K. M. Bratlie, H. Lee, K. Komvopoulos, P. Yang and G. A. Somorjai, *Nano Lett.*, 2007, **7**, 3097–3101.
6 W. F. Lin, P. A. Christensen, A. Hamnett, M. S. Zei and G. Ertl, *J. Phys. Chem. B*, 2000, **104**, 6642–6652.
7 A. Hornung, D. Zemlyanov, M. Muhler and G. Ertl, *Surf. Sci.*, 2006, **600**, 370–379.
8 F. Su, L. Lv, F. Y. Lee, T. Liu, A. I. Cooper and X. S. Zhao, *J. Am. Chem. Soc.*, 2007, **129**, 14213–14223.
9 G. Chen, S. Desinan, R. Rosei, F. Rosei and D. Ma, *Chem. Commun.*, 2012, **48**, 8009–8011.
10 K. Qadir, S. H. Joo, B. S. Mun, D. R. Butcher, J. R. Renzas, F. Aksoy, Z. Liu, G. A. Somorjai and J. Young Park, *Nano Lett.*, 2012, **12**, 5761–5768.
11 S. Guo, X. Pan, H. Gao, Z. Yang, J. Zhao and X. Bao, *Chem.–Eur. J.*, 2010, **16**, 5379–5384.
12 C. Xiao, Z. Cai, T. Wang, Y. Kou and N. Yan, *Angew. Chem., Int. Ed.*, 2008, **47**, 746–749.
13 K. Kusada, H. Kobayashi, T. Yamamoto, S. Matsumura, N. Sumi, K. Sato, K. Nagaoka, Y. Kubota and H. Kitagawa, *J. Am. Chem. Soc.*, 2013, **135**, 5493–5496.
14 C. Koenigsmann, D. B. Semple, E. S. S. E. Tobierre and S. S. Wong, *ACS Appl. Mater. Interfaces*, 2013, **5**, 5518–5530.
15 G. Viau, R. Brayner, L. Poul, N. Chakroune, E. Lacaze, F. Fiévet-Vincent and F. Fiévet, *Chem. Mater.*, 2003, **15**, 486–494.
16 M. Guerrero, Y. Coppel, N. T. T. Chau, A. Roucoux, A. Denicourt-Nowicki, E. Monflier, H. Bricout, P. Lecante and K. Philippot, *ChemCatChem*, 2013, DOI: 10.1002/cctc.20130467.
17 A. Duteil, R. Queau, B. Chaudret, R. Mozel, C. Roucau and J. S. Bradley, *Chem. Mater.*, 1993, **5**, 341–347.
18 P. Lara, K. Philippot and B. Chaudret, *ChemCatChem*, 2013, **5**, 28–45.
19 M. H. G. Prechtl, J. D. Scholten and J. Dupont, *J. Mol. Catal. A: Chem.*, 2009, **313**, 74–78.
20 V. Hulea, D. Brunel, A. Galarneau, K. Philippot, B. Chaudret, P. J. Kooyman and F. Fajula, *Microporous Mesoporous Mater.*, 2005, **79**, 185–194.
21 H. Liang, G. Chen, S. Desinana, R. Rosei, F. Rosei and D. Ma, *Int. J. Hydrogen Energy*, 2012, **37**, 17921–17927.
22 M. V. Brink, M. A. Peck, K. L. More and J. D. Hoefelmeyer, *J. Phys. Chem. C*, 2008, **112**, 12122–12126.
23 P. Lignier, R. Bellabarba, R. P. Tooze, Z. Su, P. Landon, H. Ménard and W. Zhou, *Cryst. Growth Des.*, 2012, **12**, 939–942.
24 D. Marquardt, C. Vollmer, R. Thomann, P. Steurer, R. Mulhaupt, E. Redel and C. Janiak, *Carbon*, 2011, **49**, 1326–1332.
25 W. Tu and H. Liu, *J. Mater. Chem.*, 2000, **10**, 2207–2211.
26 R. B. N. Baig and R. S. Varma, *ACS Sustainable Chem. Eng.*, 2013, **1**, 805–809.
27 B. Zhang, X. Ni, W. Zhang, L. Shao, Q. Zhang, F. Girgsdies, C. Liang, R. Schlogla and D. S. Su, *Chem. Commun.*, 2011, **47**, 10716–10718.

28 Y. Xia, P. Yang, Y. Sun, Y. Wu, B. Mayers, B. Gates, Y. Yin, F. Kim and H. Yan, *Adv. Mater.*, 2003, **15**, 353–389.
29 S. Ghosh, M. Ghosh and C. N. R. Rao, *J. Cluster Sci.*, 2007, **18**, 97–111.
30 A. Ponrouch, S. Garbarino, S. Pronovost, P.-L. Taberna, P. Simon and D. Guay, *J. Electrochem. Soc.*, 2010, **157**, K59–K65.
31 I. Pastoriza-Santos, R. A. Alvarez-Puebla and L. M. Liz-Marzan, *Eur. J. Inorg. Chem.*, 2010, 4288–4297.
32 A.-X. Yin, W.-C. Liu, J. Ke, W. Zhu, J. Gu, Y.-W. Zhang and C.-H. Yan, *J. Am. Chem. Soc.*, 2012, **134**, 20479–20489.
33 H. Liu, J. Qu, Y. Chen, J. Li, F. Ye, J. Y. Lee and J. Yang, *J. Am. Chem. Soc.*, 2012, **134**, 11602–11610.
34 J.-E. Macdonald, M. B. Sadan, L. Houben, I. Popov and U. Banin, *Nat. Mater.*, 2010, **9**, 810.
35 J. Watt, C. Yu, S. L. Y. Chang, S. Cheong and R. D. Tilley, *J. Am. Chem. Soc.*, 2013, **135**, 606–609.
36 Z. Sun, X. Wang, Z. Liu, H. Zhang, P. Yu and L. Mao, *Langmuir*, 2010, **26**, 12383–12389.
37 F. Muench, S. Kaserer, U. Kunz, I. Svoboda, J. Brötz, S. Lauterbach, H.-J. Kleebe, C. Roth and W. Ensinger, *J. Mater. Chem.*, 2011, **21**, 6286–6291.
38 C. Koenigsmann and S. S. Wong, *Energy Environ. Sci.*, 2011, **4**, 1161–1176.
39 X. Zhou, Y. Gan, J. Du, D. Tian, R. Zhang, C. Yang and Z. Dai, *J. Power Sources*, 2013, **232**, 310–322.
40 A. Takai, T. Saida, W. Sugimoto, L. Wang, Y. Yamauchi and K. Kuroda, *Chem. Mater.*, 2009, **21**, 3414–3423.
41 G. Chen, S. Desinan, R. Nechache, R. Rosei, F. Rosei and D. Ma, *Chem. Commun.*, 2011, **47**, 6308–6310.
42 P. Kluson and L. Cerveny, *Appl. Catal., A*, 1995, **128**, 13–31.
43 C. Liang, Z. Wei, Q. Xin and C. Li, *Appl. Catal., A*, 2001, **208**, 193–201.
44 G. Chen, S. Desinan, R. Rosei, F. Rosei and D. Ma, *Chem.–Eur. J.*, 2012, **18**, 7925–7930.
45 S. H. Joo, J. Y. Park, J. R. Renzas, D. R. Butcher, W. Huang and G. A. Somorjai, *Nano Lett.*, 2010, **10**, 2709–2713.
46 J. Kang, S. Zhang, Q. Zhang and Y. Wang, *Angew. Chem., Int. Ed.*, 2009, **48**, 2565–2568.
47 S. Alayoglu, A. U. Nilekar, M. Mavrikakis and B. Eichhorn, *Nat. Mater.*, 2008, **7**, 333–338.